Available online at www.sciencedirect.com

ScienceDirect

Ceramics International 40 (2014) 791–797

CERAMICS INTERNATIONAL

www.elsevier.com/locate/ceramint

External short circuit-assisted proton conducting ceramic membrane for H_2 permeation

Kun Zhang[a], Jaka Sunarso[b], Gia Hung Pham[a], Shaobin Wang[a], Shaomin Liu[a,*]

[a]*Department of Chemical Engineering & Fuels and Energy Technology Institute, Curtin University, Perth WA 6845, Australia*
[b]*Institute for Frontier Materials, Deakin University, Burwood, Victoria 3125, Australia*

Received 29 April 2013; received in revised form 19 June 2013; accepted 19 June 2013
Available online 3 July 2013

Abstract

Hydrogen permeation membrane is one of the key technologies enabling sustainable hydrogen production from hydrocarbon resources. The employment of such a membrane reactor allows simultaneous coupling of reaction and separation in one unit. This work studied the hydrogen permeation performance of external short circuit-assisted proton conducting $BaZr_{0.1}Ce_{0.2}Y_{0.7}O_{3-\delta}$ (BZCY) and $BaZr_{0.3}Ce_{0.6}Y_{0.1}Zn_{0.05}O_{3-\delta}$ (BZCYZn) perovskite membranes. In general, the lower electronic conductivity of these proton conducting perovskite membranes restricts the overall transport process. As such, we hypothesize that an external short circuit may be employed to provide the necessary electronic conductivity and thus improve the overall transport performance. Experimental results confirmed that the use of an external short circuit can improve the H_2 fluxes through the proton conducting membranes. The presence of water vapor in the feed and the permeate stream also improved the fluxes slightly, probably due to the enhanced surface exchange processes on the membrane surface. To probe the practical value of both membranes, permeation tests for four hours were carried out in different gas conditions at high temperature. The test results demonstrated BZCYZn has superior stability with respect to BZCY.

Keywords: D. Perovskite; Ceramic membrane; H_2 production; Proton conductor

1. Introduction

Clean and high efficient energy conversion technology is highly relevant towards resolving our universal energy problem in a sustainable way e.g. how to meet constantly increasing energy demands with the lowest impact to the environment. The fuel cell is one such technology which converts chemical energy into electrical energy via chemical reactions (on electrodes) and ionic transport (in electrolytes) [1,2]. Among various fuel cells, proton exchange membrane fuel cells (PEMFCs) and solid oxide fuel cells (SOFCs) are perhaps the most practical ones for stationary and transport applications [3–5]. As a fuel for these devices, hydrogen is rendered an excellent candidate given its high energy density and non-polluting reaction products (e.g. water) [6–8]. This, of course, is based solely on a perspective of hydrogen as an energy carrier. At the moment, hydrogen cannot be sustainably produced or freely found in nature in useful quantities, not to mention the daunting problems in its distribution and storage [9,10]. While hydrogen can be obtained from water using electrochemical or photochemical water splitting technologies, these processes are not practical due to the associated energy penalty and/or efficiency issue. At present, most hydrogen is produced through methane steam reforming with the reaction below [11]

$$CH_4(g) + 2H_2O \rightarrow 3H_2(g) + CO_2(g) \quad (1)$$

The drawback of this process lies in the production of carbon dioxide which should be separated from the other gases and properly treated to counteract its greenhouse effects.

Membrane technology has drawn much attention because of its numerous attractive characteristics such as low capital investment, low operating and maintenance costs, simple installation

*Corresponding author. Tel.: +61 8 9266 9056; fax: +61 8 9266 2681.
E-mail address: Shaomin.Liu@curtin.edu.au (S. Liu).

0272-8842/$ - see front matter © 2013 Elsevier Ltd and Techna Group S.r.l. All rights reserved.
http://dx.doi.org/10.1016/j.ceramint.2013.06.069

and operation and more importantly, the potential of enabling simultaneous separation and reaction capability (e.g. membrane reactors) [12,13]. Therefore, a direct dehydrogenation reaction without carbon dioxide emission can be achieved. Palladium (Pd) based metal membrane was widely employed and studied as a hydrogen permeation membrane due to its relatively high permeability and catalytic activity (to dissociate molecular hydrogen) [14]. However, its high cost and poor chemical stability towards hydrogen embrittlement have hindered its widespread use [15,16]. Proton conducting perovskite oxide is an attractive alternative of membrane reactor material for hydrogen production [17,18]. Numerous proton conducting materials have been developed since the pioneering work by Iwahara et al. with the finding of the doped $SrCeO_3$ which features proton conductivity at high temperatures [19–34]. To be applied as hydrogen permeation membrane, the materials should exhibit mixed proton and electron conducting capability [35]. Accordingly, the downside of these perovskites is in their much lower electronic conductivity relative to their proton conductivity, which rather favors their use as an electrolyte than as a hydrogen membrane [36–39]. As a consequence, the hydrogen permeation rate through these proton conducting membranes are mainly determined by electron transport across the membrane. Toward this, the electronic conductivity may be enhanced by introducing multivalent cations into $BaCeO_3$-based oxides or by adding a pure electron conducting phase (e.g. metal) into the original proton conducting perovskite phase. Indeed, enhanced hydrogen permeation fluxes were achieved in the latter case e.g. by using a dual-phase mixed conducting membrane [40–44]. In the dual-phase case however electronic conductivity improvement was obtained at the expense of a reduced amount of proton conductivity.

In this work, the purpose was to examine the hypothesis that an external short circuit structure based on the $BaZr_{0.1}Ce_{0.2}Y_{0.7}O_{3-\delta}$ and $BaZr_{0.3}Ce_{0.6}Y_{0.1}Zn_{0.05}O_{3-\delta}$ proton conducting membrane would facilitate the electron transport between the opposite sides of the membrane without altering (or reducing) the intrinsic proton conductivity. More details into this concept for oxygen separation are available elsewhere [45,46] and now we will apply it to hydrogen separation. To this end, we systematically studied the hydrogen permeation properties of the resultant proton conducting perovskite membranes.

2. Experimental

$BaZr_{0.1}Ce_{0.2}Y_{0.7}O_{3-\delta}$ (BZCY) and $BaZr_{0.3}Ce_{0.6}Y_{0.1}Zn_{0.05}O_{3-\delta}$ (BZCYZn) perovskite oxides were synthesized using a combined ethylenediaminetetraaceticacid (EDTA)-citrate complexing route. $Ba(NO_3)_2 \cdot xH_2O$, $Ce(NO_3)_2 \cdot xH_2O$, $Zr(NO_3)_4 \cdot xH_2O$, $Y(NO_3)_3 \cdot xH_2O$ and $Zn(NO_3)_2 \cdot xH_2O$ (all in analytical reagent grade), were applied as raw materials for the metal-ion sources. To precisely control the stoichiometric amount (of the metal ions), the metal nitrates were first made into their respective aqueous solutions (~1 M). The real molarity was then determined using EDTA titration technique as detailed elsewhere [20]. The desirable molar ratios were obtained by mixing the required volume of each of the metal ion solution with the known molarity, followed by adding EDTA and citric acid as the complexing agents at the molar ratio of total metal ions: EDTA: citric acid = 1: 1: 2. Ammonia solution, NH_3(aq) was added to control the solution pH to ~6. The solution was stirred afterwards during which the formation of homogeneous mixture was indicated by transparent color. Continuous heating at 90 °C led to water evaporation and later on, a transparent purple gel formation, which was then pre-fired at 250 °C, followed by calcination at 1000 °C in air for 5 h.

The synthesized oxide powders were pressed into disks using a stainless steel die and pellet press set (15.0 mm in diameter) under a hydraulic pressure of~1.5×10^8 Pa. These disks (defined as green disk membranes) (~1.0 mm in thickness) were then sintered in a muffle furnace at 1500 °C in air for 5 h using a ramping and cooling rate between 1–2 °C min^{-1}. Silver (Ag) paste was coated throughout the disk circumference to enable electrical conduction between the opposite sides of disk membrane. Platinum slurry was also coated on the opposing sides of the disk membrane. The coated disk membranes were then calcined at 800 °C in air for 2 h to increase the adherence. The setup for hydrogen permeation through the external short circuit-assisted membrane is depicted in Fig. 1.

The surface morphology of the disk membranes was obtained using scanning electron microscope (SEM, Zeiss Evo 40XVP) at an acceleration voltage of 15 kV. The powder X-ray diffraction (XRD) analysis were performed in a powder x-ray diffractometer (Bruker D8 Advances) using a Cu-Kα radiation generated at 40 kV and 30 mA.

The hydrogen permeation properties of the disk membranes were measured using a gas chromatography (GC) technique utilizing high temperature H_2 permeation apparatus. Ceramic paste was used as sealant to fix the disk membrane onto a quartz tube. The effective area for permeation is~0.45 cm^2. Argon was used as sweep gas in the permeate side to create hydrogen partial pressure gradient across the membrane. Nitrogen diluted hydrogen (50 vol% H_2 in N_2) was used as feed gas. The composition of the permeating gas was characterized using gas chromatography (Agilent 6890N Network GC system with a thermal conductivity detector (TCD)

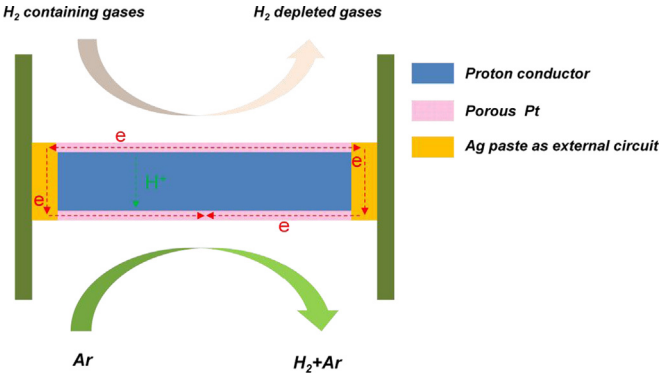

Fig. 1. Schematic presentation of the hydrogen permeation membrane utilizing proton conducting ceramics with external short circuit.

and flame ionization detector (FID)). The hydrogen permeation flux could then be calculated according to

$$J_{H_2} = \frac{F}{S}(y_{H_2} - y_{N_2}) \quad (2)$$

where F, S, y_{H2} and y_{N2} are the flow rate of the permeate, the effective membrane area, the hydrogen and nitrogen mole fraction in the permeate, respectively.

3. Results and discussion

The surface and cross-section morphology of $BaZr_{0.1}Ce_{0.2}Y_{0.7}O_{3-\delta}$ (BZCY) and $BaZr_{0.3}Ce_{0.6}Y_{0.1}Zn_{0.05}O_{3-\delta}$ (BZCYZn) disk membranes are depicted in Fig. 2, all of which demonstrate the formation of dense structures containing a small number of closed pores. Noteworthy is that such a porous structure in the bulk is not favorable for ion diffusion. Hydrogen permeation performances of 1-mm thick disk membranes of BZCY and BZCYZn between 700 and 900 °C using 50 vol% of H_2 in N_2 as feed gas and Ar as sweep gas are depicted in Fig. 3. As a reference for comparison, the performance of the basic BZCY and BZCYN disk membranes without an external short circuit e.g. silver coating in circumference and platinum coating on both opposing disk surfaces was also displayed. The temperature activated nature of the hydrogen permeation process is evident from the steady increase of all hydrogen permeation fluxes with temperature rise due to the enhanced hydrogen reduction and/or oxidation on membrane surface as well as accelerated proton diffusion in bulk membrane. BZCY has high proton conductivity and is regarded as one of the best proton conductors among perovskite type-$BaCeO_3$ and $BaZrO_3$ based materials. Nonetheless, the observed hydrogen flux through basic BZCY membrane was quite low e.g. only ~0.013 ml cm^{-2} min^{-1} at 900 °C. We speculate that this low flux is ascribed to the low electronic conductivity of BZCY. During hydrogen permeation, electrons are continuously depleted or generated when the proton was converted to hydrogen (and vice versa). As a result, the low electronic conductivity may limit the hydrogen permeation flux if it is not sufficiently high. In BZCY case, the presence of transition metal Ce allows partial reduction of some Ce^{4+} to Ce^{3+} and therefore promotes electron transfer by increasing the concentration of electronic transport carriers, i.e., electron holes.

Accordingly, the hydrogen permeation flux is also observed through the BZCYZn membrane, although at a lower value of

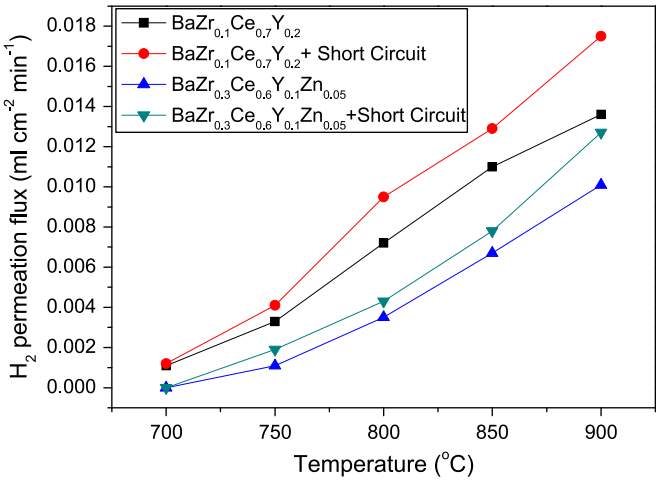

Fig. 3. Temperature dependent hydrogen permeation fluxes through basic and external short circuit-assisted $BaZr_{0.1}Ce_{0.2}Y_{0.7}O_{3-\delta}$ and $BaZr_{0.3}Ce_{0.6}Y_{0.1}Zn_{0.05}O_{3-\delta}$ membranes. Feed gas: 40 ml min^{-1} H_2+40 ml min^{-1} N_2; Sweep gas: 100 ml min^{-1} Ar.

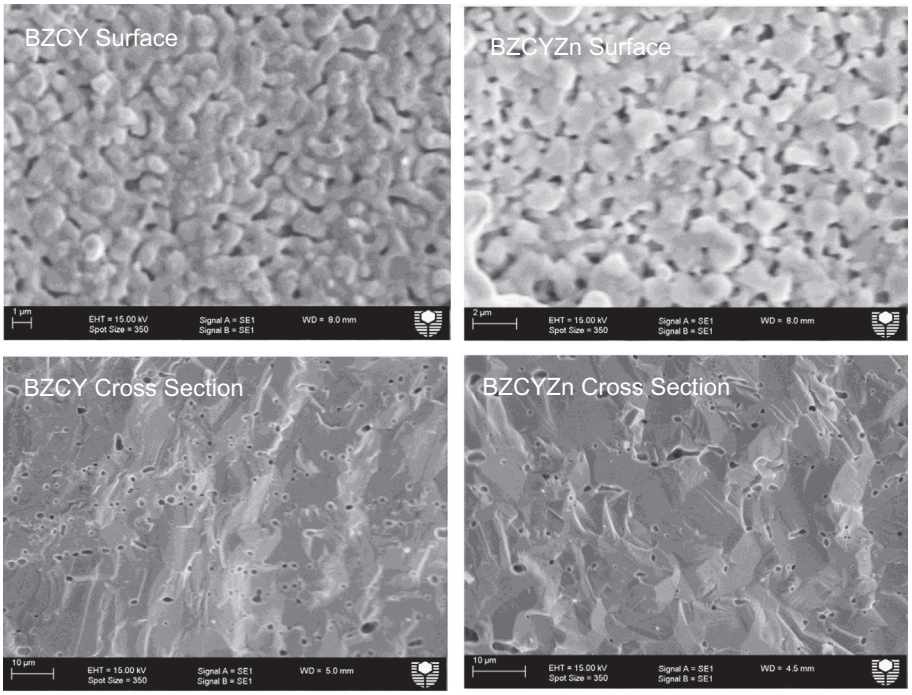

Fig. 2. SEM images of the surface and the cross-section of $BaZr_{0.1}Ce_{0.2}Y_{0.7}O_{3-\delta}$ and $BaZr_{0.3}Ce_{0.6}Y_{0.1}Zn_{0.05}O_{3-\delta}$ membranes.

~0.010 ml cm^{-2} min^{-1} at 900 °C. This lower hydrogen flux is mainly due to the relative weak proton conducting ability of BZCYZn oxide. However, the advantage of BZCYZn is not in terms of its permeation flux but rather about the stability as the presence of more Zr in the membrane has been associated with enhanced structure stability on the perovskite oxides [47–49]. It is worthwhile to trade-off some flux values with stability so that the materials can operate longer, which translates to higher reliability and low maintenance cost.

Upon utilizing external short-circuit, the hydrogen fluxes through BZCY increased by ~38% to 0.018 ml cm^{-2} min^{-1} at 900 °C whereas that through BZCYZn increased by ~20% to 0.012 ml cm^{-2} min^{-1} at 900 °C. This, to some extent, might be taken as supporting evidence towards our rationale of electronic conductivity restricting transport. External short circuit, in this respect, contributed to the enhancement of the electronic conductivity which in turn, improved the hydrogen transport rate.

Fig. 4 shows the hydrogen permeation flux through the external short circuit-assisted BZCY and BZCYZn disk membrane at 950 °C as a function of argon sweep flow rate between 50 and 200 ml min^{-1}. Hydrogen fluxes were very slightly increased with increasing sweep flow rate considering the higher partial pressure driving force across the membrane due to lower hydrogen partial pressure at the permeate side (at higher sweep flow rate). The very slight nature of increase implies less dependence of hydrogen transport towards sweep gas flow rate. For example at 950 °C, when the sweep flow rate was raised by 400% from 50 ml min^{-1} to 200 ml min^{-1}, the flux through BZCY was only improved by 25% (from 0.0112 ml cm^{-2} min^{-1} to 0.0141 ml cm^{-2} min^{-1}) while the flux through BZCYN was only improved by 26% from 0.0072 to 0.0091 ml cm^{-2} min^{-1}.

The effect of water vapor on the hydrogen permeation transport operated between 700 and 900 °C was probed by the addition of 3% of water vapor into both sides of sweep gas and feed gas; the results of which is depicted in Fig. 5. The hydrogen fluxes of external short circuit-assisted BZCY and BZCYZn disk membranes are slightly increased with the addition of water vapor, which implies reduced hydrogen transport resistance within the membrane system. To further test the possible mechanism of how water effects the hydrogen permeation through the ceramic membranes, 3 vol% H_2O was added into both sides of the membrane reactor while hydrogen flow was stopped e.g. resulting in the observation that no hydrogen flux could be detected in both sides of the membrane reactor. This highlights the fact that water vapor by itself without proper catalyst could not dissociate into appreciable hydrogen ions and associated into hydrogen gas. The presence of water vapor is likely to reduce the activation energy for proton transformation to hydrogen atoms (and vice versa) taking place on the membrane surfaces [21]. The possible reaction mechanism for hydrogen flux improvement in the presence of water vapor is proposed as follows:

1. at the feed side of the membrane

$$H_2(g) + H_2O(g) \rightarrow H_3O^+ + H^+ + 2e^- \quad (3)$$

2. at the permeate side of the membrane

$$2H^+ + 2H_2O(g) + 2e \rightarrow 2H_3O^+ + 2e \rightarrow H_2(g) + 2H_2O(g) \quad (4)$$

The presence of water vapor can assist the hydrogen and proton exchange processes playing a role of catalyst. In comparison with the surface reaction in a drying state, these intermediate steps likely reduce the activation energy of the exchange processes and thus improve the reaction kinetics contributing the higher H_2 flux. In addition, water may also increase proton conductivity through membrane as illustrated by Eq. (5) [50].

$$H_2O + V_O^{\cdot\cdot} \leftrightarrow O_O^x + 2H^+ \quad (5)$$

For practical applications, stability is critical. Most perovskite type proton conducting membranes are very sensitive and

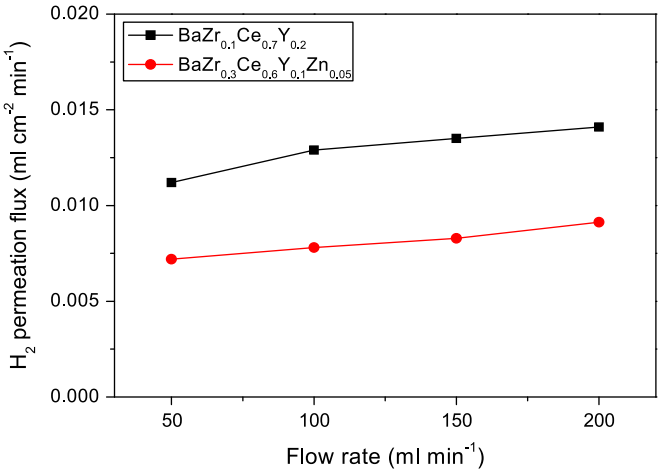

Fig. 4. Hydrogen permeation fluxes through external short circuit-assisted $BaZr_{0.1}Ce_{0.2}Y_{0.7}O_{3-\delta}$ and $BaZr_{0.3}Ce_{0.6}Y_{0.1}Zn_{0.05}O_{3-\delta}$ membranes at 950 °C and different sweep gas flow rates.

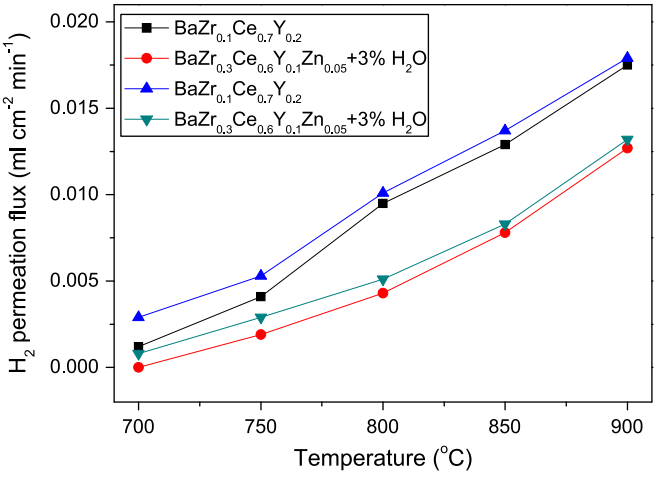

Fig. 5. Temperature dependent hydrogen permeation fluxes through external short circuit-assisted $BaZr_{0.1}Ce_{0.2}Y_{0.7}O_{3-\delta}$ and $BaZr_{0.3}Ce_{0.6}Y_{0.1}Zn_{0.05}O_{3-\delta}$ membranes on both membrane sides with and without water vapor (3 vol% H_2O).

reactive in the presence of acidic gases such as CO_2 due to their intrinsic alkaline composition. The stability of the permeation fluxes of the external short circuit-assisted BZCY and BZCYZn disk membranes in the presence of CO_2 is tested by adding 10 vol% of CO_2 in Ar as sweep gas after 4 h of normal testing with the results displaying in Fig. 6. The permeation flux profile was quite stable in the initial 4 h when Ar was used as sweep gas. Sudden rapid decline of hydrogen flux occurred on both membranes when 10 vol% CO_2 was introduced. Later on, when the sweep gas was switched to Ar again, the hydrogen flux of BZCY slightly increased, but far less than its original value. BZCYZn disk membrane, in contrast, recovered almost all of its original flux value before CO_2 introduction; denoting its superior stability to resist CO_2. In some cases of the oxygen permeation membranes with the existence of CO_2 gas, similar phenomena were observed. It has been proven that the physical adsorption of CO_2 has an effect on the oxygen vacancies of the membrane surface, rather than a chemical reaction with the membrane surface to form carbonate, which could lead to the immediate decrease in oxygen fluxes [51,52]. Therefore, in this case, the immediate decline of hydrogen flux through BZCYZn may be also due to the absorption effect of CO_2 on the membrane surface, which occupies the active sites around the oxygen vacancies and thus inhibits hydrogen association and desorption. As further evidence, Fig. 7 shows the powder XRD patterns of BZCY and BZCYZn disk membranes before and after the stability test. In case of BZCY, it is evident that after the test, the original characteristic peaks from the fresh sample were no longer preserved with the main peak (e.g. the one at 28°) shifted to a lower angle accompanied by the presence of extra peaks distinct to those before the test. These observations suggest the deterioration and/or substantial modification of the original crystal structure as well as the formation of barium carbonate or others due to reaction with CO_2. In case of BZCYZn, the characteristic peaks from before the test were retained after the test.

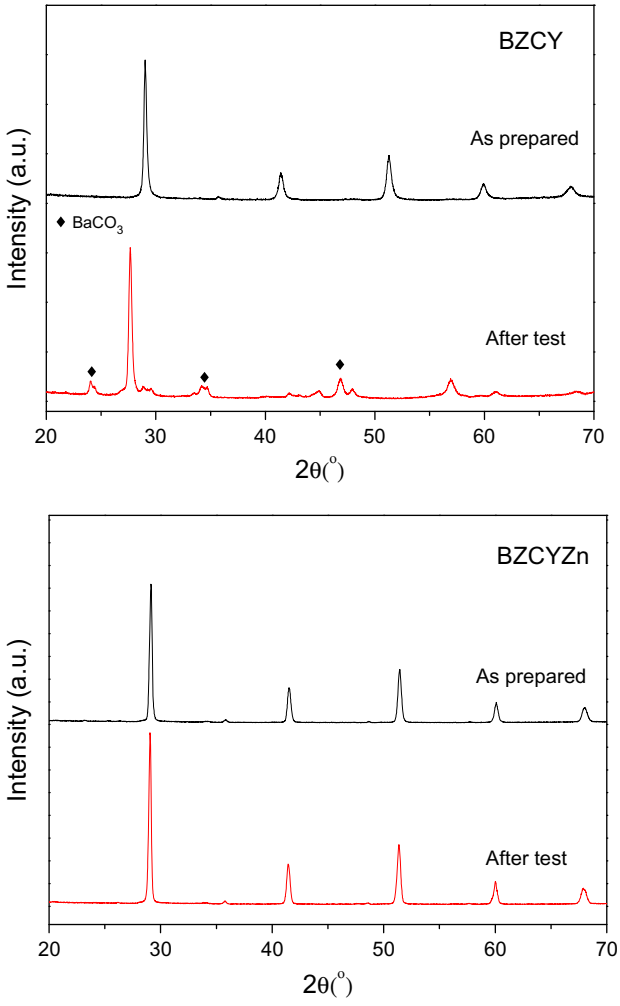

Fig. 7. XRD patterns of $BaZr_{0.1}Ce_{0.2}Y_{0.7}O_{3-\delta}$ and $BaZr_{0.3}Ce_{0.6}Y_{0.1}Zn_{0.05}O_{3-\delta}$ membrane before/after the stability test under pure CO_2 with flow rate of 20 ml min^{-1} for 10 h at 850 °C.

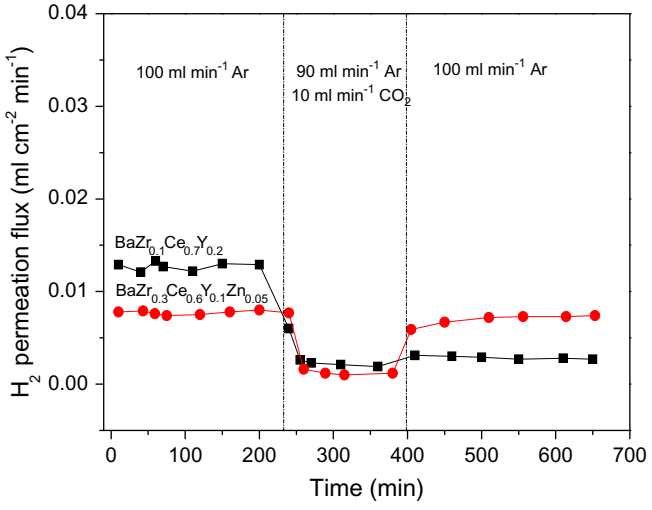

Fig. 6. Long term hydrogen permeation fluxes through $BaZr_{0.1}Ce_{0.2}Y_{0.7}O_{3-\delta}$ and $BaZr_{0.3}Ce_{0.6}Y_{0.1}Zn_{0.05}O_{3-\delta}$ membranes (with external short circuit) using different sweep gas at 850 °C.

4. Conclusions

$BaZr_{0.1}Ce_{0.2}Y_{0.7}O_{3-\delta}$ (BZCY) and $BaZr_{0.3}Ce_{0.6}Y_{0.1}Zn_{0.05}O_{3-\delta}$ (BZCYZn) disk membranes have been prepared using the EDTA-citrate route and sintering at 1500 °C. Utilizing the external short circuit concept, the performance of these membranes for H_2 permeation was studied. H_2 permeation fluxes through BZCY and BZCYZn membranes assisted with an external short circuit were higher than those through basic BZCY and BZCYZn membranes. Addition of water vapor into the sweep gas led to a slight increase of H_2 permeation fluxes for both membranes, most likely due to water vapor's role to facilitate hydrogen adsorption and/or an association process. In the presence of CO_2, BZCYZn demonstrated superior structure and permeation flux stability e.g. retaining the original structure from before the test and recovering the original flux from the normal test before the introduction of CO_2. Further studies into BZCYZn are thus warranted with the aim to optimize its H_2 flux using thin film technology.

Acknowledgment

The authors appreciate the financial support provided by the Australian Research Council through the Future Fellow Program (FT12100178).

References

[1] E.D. Washsman, K.T. Lee, Lowering the temperature of solid oxide fuel cells, Science 334 (2011) 935–939.
[2] B.C.H. Steele, A. Heinzel, Materials for fuel-cell technologies, Nature 414 (2001) 345–352.
[3] Z.L. Zhan, S.A. Barnett, An octane-fueled solid oxide fuel cell, Science 308 (2005) 844–847.
[4] Z. Shao, S.M. Haile, A high-performance cathode for the next generation of solid-oxide fuel cells, Nature 43 (2004) 170–173.
[5] M.K. Debe, Electrocatalyst approaches and challenges for automotives fuel cells, Nature 486 (2012) 43–51.
[6] M.Z. Jacobson, W.G. Colella, Cleaning the air and improving health with hydrogen fuel-cell vehicles, Science 308 (2005) 1901–1905.
[7] D.L. Trimm, Z.I. Önsan, Onboard fuel conversion for hydrogen-fuel-cell driven vehicles, Catalysis Reviews 43 (2001) 31–84.
[8] J.M. Ogden, M.M. Steinbugler, T.G. Kreutz, A comparison of hydrogen, methanol and gasoline as fuels for fuel cell vehicles: implications for vehicle design and infrastructure development, Journal of Power Sources 79 (1999) 143–148.
[9] D.K. Ross, Hydrogen storage: the major technological barrier to the development of hydrogen fuel cell cars, Vacuum 80 (2006) 1084–1089.
[10] J.A. Turner, Sustainable hydrogen production, Science 305 (2004) 972–974.
[11] L. Barelli, G. Bidini, F. Gallorini, S. Servili, Hydrogen production through sorption-enhanced steam methane reforming and membrane technology: a review, Energy 33 (2008) 554–570.
[12] Y. Wei, W. Yang, J. Caro, H. Wang, Dense ceramic oxygen permeable membranes and catalytic membrane reactors, Chemical Engineering Journal 220 (2013) 185–203.
[13] S. Liu, X. Tan, K. Li, R. Hughes, Methane coupling using catalytic membrane reactors, Catalysis Reviews 43 (2001) 147–198.
[14] E. Kikuchi, Membrane reactor application to hydrogen production, Catalysis Today 56 (2000) 97–101.
[15] J. Tong, H. Suda, K. Haraya, Y. Matsumura, A novel method for the preparation of thin dense Pd membrane on macroporous stainless steel tube filter, Journal of Membrane Science 260 (2005) 10–18.
[16] S. Yun, S.T. Oyama, Correlations in palladium membrane membranes for hydrogen separation: a review, Journal of Membrane Science 375 (2011) 28–45.
[17] H. Iwahara, Y. Asakura, K. Katahira, M. Tanaka, Prospect of hydrogen technology using proton-conducting ceramics, Solid State Ionics 168 (2004) 299–310.
[18] H. Iwahara, Technological challenges in the application of proton conducting ceramics, Solid State Ionics 77 (1995) 289–298.
[19] H. Iwahara, T. Yajima, T. Hibino, H. Ushida, Performance of solid oxide fuel cell using proton and oxide ion mixed conductors based on $BaCe_{1-x}Sm_xO_{3-\delta}$, Journal of the Electrochemical Society 140 (1993) 1687–1691.
[20] C. Zuo, S. Zha, M. Liu, M. Hatano, M. Uchiyama, $Ba(Zr_{0.1}Ce_{0.7}Y_{0.2})O_{3-\delta}$ as an electrolyte for low-temperature solid oxide fuel cells, Advanced Materials 18 (2006) 3318–3320.
[21] K.D. Kreuer, Proton-conducting oxides, Annual Review of Materials Science 33 (2003) 333–359.
[22] Y. Lin, R. Ran, Y. Guo, W. Zhou, R. Cai, J. Wang, Z. Shao, Proton-conducting fuel cells operating on hydrogen, ammonia and hydrazine at intermediate temperatures, International Journal of Hydrogen Energy 35 (2010) 2637–2642.
[23] Y. Lin, W. Zhou, J. Sunarso, R. Ran, Z. Shao, Characterization and evaluation of $BaCo_{0.7}Fe_{0.2}Nb_{0.1}O_{3-\delta}$ as a cathode for proton-conducting solid oxide fuel cells, International Journal of Hydrogen Energy 37 (2012) 484–497.
[24] F. Zhao, S. Wang, L. Dixon, F. Chen, Novel $BaCe_{0.7}In_{0.2}Yb_{0.1}O_{3-\delta}$ proton conductor as electrolyte for intermediate temperature solid oxide fuel cells, Journal of Power Sources 196 (2011) 7500–7504.
[25] F. Zhao, Q. Liu, S. Wang, K. Brinkman, F. Chen, Synthesis and characterization of $BaIn0_{3-x}Y_xCe_{0.7}O_{3-\delta}$ ($x=0$, 0.1, 0.2, and 0.3) proton conductors, International Journal of Hydrogen Energy 35 (2010) 4258–4263.
[26] G. Meng, G. Ma, Q. Ma, R. Peng, X. Liu, Ceramic membrane fuel cells based on solid proton electrolytes, Solid State Ionics 178 (2007) 697–703.
[27] K. Xie, R. Yan, Y. Jiang, X. Liu, G. Meng, A simple and easy one-step fabrication of thin $BaZr_{0.1}Ce_{0.7}Y_{0.2}O_{3-\delta}$ electrolyte membrane for solid oxide fuel cells, Journal of Membrane Science 325 (2008) 6–10.
[28] Z. Sun, E. Fabbri, L. Bi, E. Traversa, Electrochemical properties and intermediate-temperature fuel cell performance of dense yttrium-doped barium zirconate with calcium addition, Journal of the American Ceramic Society 95 (2012) 627–635.
[29] Y. Liu, Y. Guo, R. Ran, Z. Shao, A new neodymium-doped $BaZr_{0.8}Y_{0.2}O_{3-\delta}$ as potential electrolyte for proton-conducting solid oxide fuel cells, Journal of Membrane Science 415 (2012) 391–398.
[30] X. Tan, J. Song, X. Meng, B. Meng, Preparation and characterization of $BaCe_{0.95}Tb_{0.05}O_{3-\delta}$ hollow fiber membranes for hydrogen permeation, Journal of the European Ceramic Society 32 (2012) 2351–2357.
[31] A. Thursfield, A. Murugan, R. Franca, I.S. Metcalfe, Chemical looping and oxygen permeable ceramic membranes for hydrogen production-a review, Energy and Environmental Science 5 (2012) 7421–7459.
[32] Y. Liu, X. Tan, K. Li, $SrCe_{0.95}Yb_{0.05}O_{3-\delta}$ hollow-fiber membrane and its property in proton conduction, AIChE Journal 52 (2006) 1577–1585.
[33] L. Malavasi, C.A.J. Fisher, M.S. Islam, Oxide-ion and proton conducting electrolyte materials for clean energy applications: structural and mechanistic features, Chemical Society Reviews 39 (2010) 4370–4387.
[34] G.C. Mather, D. Poulidi, A. Thursfield, M.J. Pascual, J.R. Jurado, I.S. Metcalfe, Hydrogen-permeable characteristics of a $SrCeO_3$-based ceramic separation membrane: thermal, ageing and surface-modification effects, Solid State Ionics 181 (2010) 230–235.
[35] T. Norby, Y. Larring, Mixed hydrogen ion-electronic conductors for hydrogen permeable membranes, Solid State Ionics 136 (2000) 139–148.
[36] L. Zhao, B. He, Y. Ling, Z. Xun, R. Peng, G. Meng, X. Liu, Cobalt-free oxide $Ba_{0.5}Sr_{0.5}Fe_{0.8}Cu_{0.2}O_{3-\delta}$ for proton-conducting solid oxide fuel cell cathode, International Journal of Hydrogen Energy 35 (2010) 3769–3774.
[37] L. Zhao, B. He, B. Lin, H. Ding, S. Wang, Y. Ling, R. Peng, G. Meng, X. Liu, High performance of proton-conducting solid oxide fuel cell with a layered $PrBaCo_2O_{5+\delta}$ cathode, Journal of Power Sources 194 (2009) 835–837.
[38] L. Bi, S. Zhang, S. Fang, L. Zhang, H. Gao, G. Meng, W. Liu, In situ fabrication of a supported $Ba_3Ca_{1.18}Nb_{1.82}O_{9-\delta}$ membrane electrolyte for a proton-conducting SOFC, Journal of the American Ceramic Society 91 (2008) 3806–3809.
[39] L. Yang, S. Wang, K. Blinn, M. Liu, Z. Liu, Z. Cheng, M. Liu, Enhanced sulfur and coking tolerance of a mixed ion conductor for SOFCs: $BaZr_{0.1}Ce_{0.7}Y_{0.2-x}Yb_xO_{3-\delta}$, Science 326 (2009) 126–129.
[40] M. Cai, S. Liu, K. Efimov, J. Caro, A. Feldhoff, H. Wang, Preparation and hydrogen permeation of $BaCe_{0.95}Nd_{0.05}O_{3-\delta}$ membranes, Journal of Membrane Science 343 (2009) 90–96.
[41] X. Meng, J. Song, N. Yang, B. Meng, X. Tao, Z. Ma, K. Li, Ni–$BaCe_{0.95}Tb_{0.05}O_{3-\delta}$ cermet membrane for hydrogen permeation, Journal of Membrane Science 401 (2012) 300–305.
[42] C. Zuo, S.E. Dorris, U. Balachandran, M. Liu, Effect of Zr-doping on the chemical stability and hydrogen permeation of the Ni–$BaCe_{0.8}Y_{0.2}O_{3-\delta}$ mixed protonic-electronic conductor, Chemistry of Materials 18 (2006) 4647–4650.
[43] C. Zuo, T.H. Lee, S.E. Dorris, U. Balachandran, M. Liu, Composite Ni–$Ba(Zr_{0.1}Ce_{0.7}Y_{0.2})O_{3-\delta}$ membrane for hydrogen separation, Journal of Power Source 159 (2006) 1291–1295.

[44] X. Qi, Y.S. Lin, Electrical conducting properties of proton-conducting terbium-doped strontium cerate membrane, Solid State Ionics 120 (1999) 85–93.

[45] K. Zhang, Z. Shao, C. Li, S. Liu, Novel CO_2-tolerant ion-transporting ceramic membranes with an external short circuit for oxygen separation at intermediate temperatures, Energy and Environmental Science 5 (2012) 5257–5264.

[46] K. Zhang, Y. Zou, C. Su, Z. Shao, L. Liu, S. Wang, S. Liu, CO_2 and water vapor-tolerant yttria stabilized bismuth oxide (YSB) membranes with external short circuit for oxygen separation with CO_2 capture at intermediate temperatures, Journal of Membrane Science 427 (2013) 168–175.

[47] S. Li, W. Jin, P. Huang, N. Xu, J. Shi, M.Z.C. Hu, A. Payzant, Y.H. Ma, Perovskite-related ZrO_2-doped $SrCo_{0.4}Fe_{0.6}O_{3-\delta}$ membrane for oxygen permeation, AIChE Journal 45 (2009) 276–284.

[48] H. Jiang, F. Liang, O. Czuprat, K. Efimov, A. Feldhoff, S. Schirrmeister, T. Schiestel, H. Wang, J. Caro, Hydrogen production by water dissociation in surface-modified $BaCoFeZrO_{3-\delta}$ hollow fiber membrane reactor with improved oxygen permeation, Chemistry–A European Journal 16 (2010) 7898–7903.

[49] E. Fabbri, A. D'Epifanio, E.D. Bartolomeo, S. Licoccia, E. Traversa, Tailoring the chemical stability of $Ba(Ce_{0.8-x}Zr_x)Y_{0.2}O_{3-\delta}$ protonic conductors for intermediate temperature solid oxide fuel cells (IT-SOFCs), Solid State Ionics 179 (2008) 558–564.

[50] S.J. Song, E.D. Wachsman, J. Rhodes, S.E. Dorris, U. Balachandran, Hydrogen permeability of $SrCe_{1-x}M_xO_{3-\delta}$ ($x=0.05$, M=Eu, Sm), Solid State Ionics 167 (2004) 99–105.

[51] X. Tan, N. Liu, B. Meng, J. Sunarso, K. Zhang, S. Liu, Oxygen permeation behavior of $La_{0.6}Sr_{0.4}Co_{0.8}Fe_{0.2}O_3$ hollow fibre membranes with highly concentrated CO_2 exposure, Journal of Membrane Science 389 (2012) 216–222.

[52] J. Wang, Y. Wei, L. Zhou, Li Zhong, H. Wang, Oxygen permeation through a CO_2-tolerant mixed conducting oxide (Pr0.9La0.1)2 (Ni0.74Cu0.21Ga0.05)O_4+δ, AIChE Journal 58 (2012) 2473–2478.